


Research Article

ELM-Assisted Particle Filter for INS/UWB-Integrated Quadrotor Positioning

Shuhui Bi,^{1,2} Fukun Li,¹ Lei Wang,^{2,3} Yuan Xu ,^{1,4} and Jidong Feng¹

¹School of Electrical Engineering, University of Jinan, Jinan 250022, China

²Shandong Guige Intelligent Technology Co., Ltd., Jinan, Shandong Province, China

³HRG (Shandong) Intelligent Equipment Research Institute, Jinan, China

⁴Shandong Honest Credibility Electric Science and Tehcnology Co., Ltd., Dezhou, China

Correspondence should be addressed to Yuan Xu; xy_abric@126.com

Received 19 January 2022; Revised 22 April 2022; Accepted 3 May 2022; Published 13 June 2022

Academic Editor: A. M. Bastos Pereira

Copyright © 2022 Shuhui Bi et al. This is an open access article distributed under the Creative Commons Attribution License, which permits unrestricted use, distribution, and reproduction in any medium, provided the original work is properly cited.

At present, with the wide application of the quadrotor, accurate positioning has become an increasingly important problem and needs to be considered. In this study, the inertial navigation system (INS) and ultra-wideband (UWB) technology are used together to collect the flight data of the quadrotor, and the particle filter (PF) algorithm will be employed to fuse the data information of the two sensors for reducing the error and obtaining the movement path of the quadrotor in the three dimensional (3D) space. Meanwhile, for making PF work more accurate, the extreme learning machine (ELM) is adopted to map the equation of state in the filtering process to make position information more reliable. In addition, ELM can also establish a new signal through mapping when UWB's signal is interrupted, so that the whole system can work normally. To verify the effectiveness of the proposed method, a real experiment was carried out. The experimental results show that the ELM-assisted PF strategy has a good effect on INS/UWB-integrated navigation quadrotor positioning. When UWB signals are normal, compared with the single PF, the ELM-assisted PF is able to improve positioning accuracy by about 18.44%. When UWB's signal is interrupted, compared with the least square support vector machine- (LS-SVM-) assisted PF, the ELM-assisted PF could improve positioning accuracy by about 1.15 m. On the whole, the proposed design algorithm not only improves the positioning accuracy but also can predict UWB's signal when it is interrupted and thus make the filter work normally.

1. Introduction

Quadrotor aircraft can adjust its attitude in the space by changing the speed. Because of the development of modern control technology, quadrotor aircraft has been more and more widely concerned. The stable flight of the quadrotor can be used in aerial photography, rescue and search, security, fire-fighting, pesticide spraying, construction, and other high-risk operating environments [1, 2]. Therefore, how to control the moving path and space position of the quadrotor, that is, how to achieve accurate positioning of the quadrotor, is a much more important subject that needs to be considered [3–9].

The inertial navigation system measures the acceleration of the target in the reference frame and obtains velocity,

heading angle, and position information by integrating it twice over time. The inertial navigation system is based on Newtonian mechanics, which belongs to the way of calculation navigation. It has good independence and continuity, does not depend on external information, nor does it radiate energy outward, and has low requirements for the working environment. However, due to the lack of reference, the solution position of the inertial navigation system affects each other, and the error will gradually increase with time accumulation; therefore, INS is not suitable for a long period, long distance navigation, and positioning. The UWB technology obtains the position information by collecting distance information between the reference node and the motion carrier, and the positions are independent from each other, so there is no time error accumulation problem.

However, the signal transmission of the reference node is affected by the external environment, so there is the possibility of occlusion, deviation, or interruption. Therefore, it is difficult for a single navigation technology to meet the requirements of accurate positioning. For avoiding that, INS and UWB-integrated technology was proposed. Such multisensor fusion manner can give full play to their respective advantages, eliminate the error accumulation problem of INS, and ensure the continuity of signal data [10–14].

Measurement data from the sensor are subjects to various kinds of noise, such as measurement environment, measuring technology, or hardware itself. Using the appropriate filtering algorithm can suppress the influence of bad noise, improve the signal quality, and make the positioning more accurate and reliable, so as to improve the performance of the whole navigation system. The particle filter algorithm is an effective sampling method, and it approximates the density function by calculating and comparing a random sample. In this method, the sample mean replaced the integral operation. The Monte Carlo method is its central idea, and probability is expressed by the particle set, which is widely used in practice [15, 16]. In the positioning process, in order to obtain more stable and superior effects, we can also use some learning strategies to match with filtering algorithms, such as the BP neural network, ELM, and LS-SVM.

The extreme learning machine was proposed with the development of computer network technology. It was presented aiming to improve the backward propagation (BP) algorithm to improve low learning efficiency and simplify the setting of learning parameters. ELM is based on the feedforward neural network and improves the fuzzy neural network and thence has good adaptability in the supervised learning problem. In some current views, ELM has advantages in speed and generalization [17–20].

In this study, the extreme learning machine will be adopted to assist the particle filter algorithm to calibrate the INS/UWB-integrated navigation system mounted on a quadrotor. In this process, the extreme learning machine plays two roles. ELM establishes the relationship between each state value in the filtering process, so as to make the whole model more stable. By establishing the mapping relationship between INS and UWB, even UWB's signal is interrupted, and the necessary data needed for filtering can be provided to make the system work normally and improve the robustness of the whole system. In order to prove the availability of the proposed strategy, the experiment has been carried out in a real environment, and the experimental results prove the effectiveness of the proposed strategy.

The main contributions of this study are as follows:

- (i) A new PF algorithm based on the extreme learning machine is proposed to implement the fusion of INS and UWB's data, and the mapping relationship of state values in the filtering process is built by training of the extreme learning machine, which improves the reliability of the positioning system.
- (ii) The mapping between INS and UWB can be built by training of the extreme learning machine, and the

signal compensation can be carried out when UWB's signal is interrupted, so that the whole system can work normally.

The remaining construction of this study is outlined as follows. The ELM-assisted PF strategy is explained in "INS/UWB-Integrated Navigation Quadrotor Positioning Scheme," the PF filtering strategy for INS/UWB positioning and the ELM-assisted strategy are given in the "Particle Filtering Algorithm" and "The Scheme of ELM," and the real test and error analysis are completed in "Test." Finally, "Conclusion" describes the effectiveness of the proposed method for INS/UWB-integrated navigation quadrotor positioning.

2. INS/UWB-Integrated Navigation Quadrotor Positioning Scheme

The INS/UWB-integrated navigation quadrotor positioning scheme will be discussed for the following two situations.

- (i) When UWB's signal is available, INS and UWB measure the position $Po^{(I)}$ and $Po^{(U)}$ of the target quadrotor, respectively. PF makes more accurate estimate $\delta P\hat{o}$ of the position error δPo by fusing the information of $Po^{(I)}$ and $Po^{(U)}$ to correct $Po^{(I)}$ and output the optimized target position. δPo is used as the observation vector in PF. In the filtering process, ELM establishes the mapping of the state deviation $\Delta x_t, t \in [1, \infty)$ generated at each moment of PF and correct Δx by the more accurate estimate $\Delta \hat{x}$ generated by ELM to reduce the state deviation. Meanwhile, the state vector $\hat{x}_{t|t-1}, t \in [1, +\infty)$ output from PF and δPo are taken as input and targets of ELM, and ELM keeps training to establish the mapping relationship between them. The whole system works normally, and ELM plays two roles: (1) to constantly correct Δx_t along with PF, and ELM outputs deviation information; (2) through training, the mapping relationship between the Δx_t output by PF and δPo is constantly established. At this time, ELM works offline and does not output observation information. The positioning strategy is shown in Figure 1.
- (ii) When UWB's signal is interrupted, UWB cannot provide $Po^{(U)}$ and PF cannot work properly due to the lack of the observation vector δPo . At this point, ELM outputs the predicted observation vector $\delta \widehat{P\hat{o}}$ through the mapping established in the previous stage, and $\delta \widehat{P\hat{o}}$ is used as the observation vector of PF, so PF can work normally when UWB's signal is interrupted. At this time, ELM works in the prediction stage and outputs observation information. The positioning strategy is shown in Figure 2.

3. Particle Filtering Algorithm

On the basis of INS/UWB integrated navigation, we use the particle filter algorithm to fuse sensor information. The state equation of particle filter is as follows:

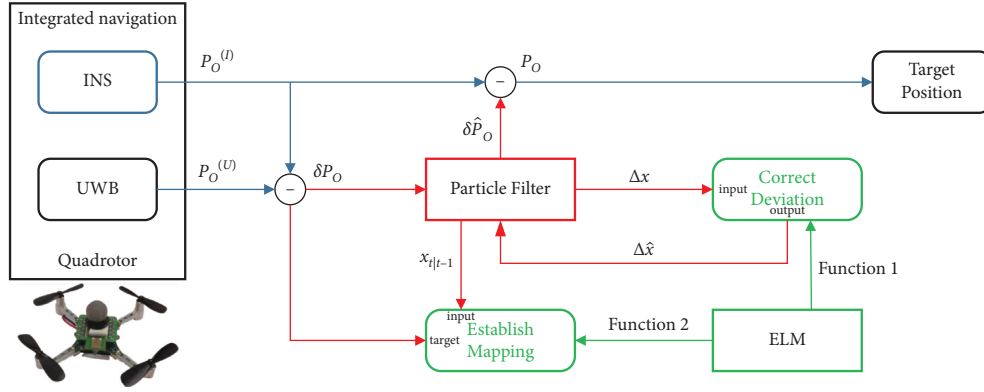


FIGURE 1: ELM-assisted PF data fusion strategy when UWB measurements are available.

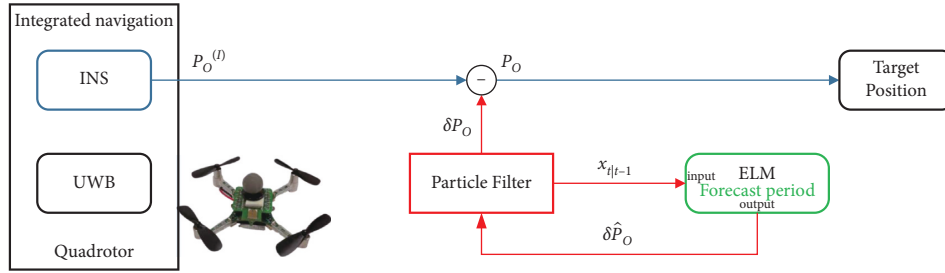


FIGURE 2: ELM-assisted PF data fusion strategy when UWB's signal is interrupted.

$$\begin{bmatrix} \phi_{t|t-1} \\ \delta V_{t|t-1}^n \\ \delta P_{t|t-1}^n \\ \nabla_{t|t-1}^b \\ \varepsilon_{t|t-1}^b \end{bmatrix}_{X_{t|t-1}} = \begin{bmatrix} I_{3 \times 3} & 0_{3 \times 3} & 0_{3 \times 3} & 0_{3 \times 3} & -I_{3 \times 3} C_b^n \Delta T \\ S(f_t^n) \Delta T & I_{3 \times 3} & 0_{3 \times 3} & I_{3 \times 3} C_b^n \Delta T & 0_{3 \times 3} \\ 0_{3 \times 3} & I_{3 \times 3} \Delta T & I_{3 \times 3} & 0_{3 \times 3} & 0_{3 \times 3} \\ 0_{3 \times 3} & 0_{3 \times 3} & 0_{3 \times 3} & I_{3 \times 3} & 0_{3 \times 3} \\ 0_{3 \times 3} & 0_{3 \times 3} & 0_{3 \times 3} & 0_{3 \times 3} & I_{3 \times 3} \end{bmatrix}_{A_t} \begin{bmatrix} \phi_{t-1} \\ \delta V_{t-1}^n \\ \delta P_{t-1}^n \\ \nabla_{t-1}^b \\ \varepsilon_{t-1}^b \end{bmatrix}_{X_{t-1}} + w_{t-1}, \quad (1)$$

$$S(f_t^n) = \begin{bmatrix} 0 & f_{Ut}^n & -f_{Nt}^n \\ -f_{Ut}^n & 0 & f_{Et}^n \\ f_{Nt}^n & -f_{Et}^n & 0 \end{bmatrix}, \quad (2)$$

$$C_b^n = \begin{bmatrix} \cos \gamma & 0 & -\sin \gamma \\ 0 & 1 & 0 \\ \sin \gamma & 0 & \cos \gamma \end{bmatrix} \begin{bmatrix} 1 & 0 & 0 \\ 0 & \cos \theta & \sin \theta \\ 0 & -\sin \theta & \cos \theta \end{bmatrix} \begin{bmatrix} \cos \psi & -\sin \psi & 0 \\ \sin \psi & \cos \psi & 0 \\ 0 & 0 & 1 \end{bmatrix}. \quad (3)$$

In (1), t is the time index, ϕ_t , δV_t^n , and δP_t^n denote the errors of the INS's attitude, velocity, and position, $(\nabla_t^b, \varepsilon_t^b)$ represent the accelerometers bias and gyroscope drift employ. ΔT is the sample time, and $w_t \sim N(0, Q_t)$ represent the noise of the system. In (2), $(f_{Ut}^n, f_{Et}^n, f_{Nt}^n)$ is the acceleration

up, east, and north of the coordinate system. In (3), C_b^n is the rotation matrix, and θ, γ, ψ represent the rotation angle around $x, y,$ and z axis.

The observation equation of the particle filter is as follows.

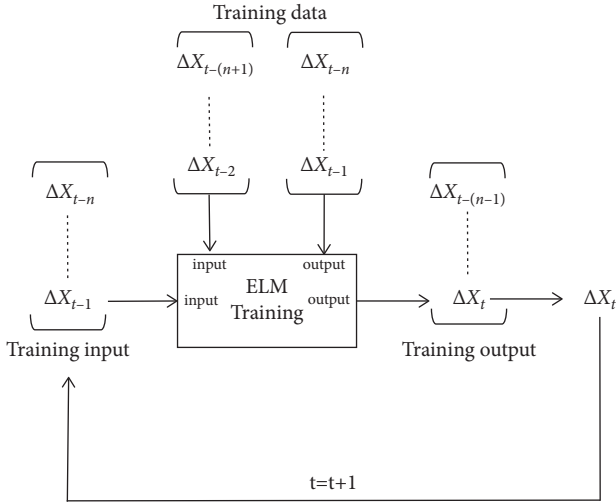


FIGURE 3: ELM training process.

$$\begin{aligned}
 Y_t &= [Y_t^{(1)} Y_t^{(2)} Y_t^{(3)} Y_t^{(4)} Y_t^{(5)} Y_t^{(6)}]^T, \\
 \underbrace{\left[\delta(d_t^{(i)})^2 \right]}_{Y_t^{(i)}} &= \left[(d_t^{(i)})^2 - (d_t^U)^2 \right] \\
 &= \frac{2(x_t^I - x_t^{(i)})\delta x_t^{(i)} + 2(y_t^I - y_t^{(i)})\delta y_t^{(i)} + 2(z_t^I - z_t^{(i)})\delta z_t^{(i)}}{g(x_{t|t-1}^{(i)})} + \frac{\gamma_{d_t^{(i)}}}{\gamma_t^{(i)}}.
 \end{aligned} \quad (4)$$

In the equation above, Y_t is the observation vector of PF, $\delta(d_t^{(i)})^2$ is the square of the difference between the distances collected by INS and UWB, $(\delta x_t^{(i)}, \delta y_t^{(i)}, \delta z_t^{(i)})$ is the filter's estimation of the INS position errors, $(x_t^{(i)}, y_t^{(i)}, z_t^{(i)})$ is the measurement position of INS, (d_t^I, d_t^U) is the distance obtained by INS and UWB, respectively, $(x_t^{(i)}, y_t^{(i)}, z_t^{(i)})$ is the position of the i^{th} RN, $\gamma_t^{(i)} \sim N(0, R^{(i)})$ is the measurement noise, t is the time index, and superscript i ($i = 1 \sim 6$) stands for the label of RN.

4. The Scheme of ELM

In the navigation positioning process, we use the PF algorithm to fuse the positioning information of the two sensors and reduce the bad noise and error. ELM is used to assist the PF algorithm. ELM has two functions here. One is to establish the mapping relationship between various state values in the PF filtering process to optimize the accuracy. The other is when UWB's measurement being interrupted; the mapping relationship between the state value and the observation value is established to compensate the signal, so that the filter can work normally and enhance the stability of the system.

4.1. Scheme 1: Correction of State Deviation in the Filtering Process. In the particle filter state update process, the state value x_{state} describes the state information of the motion quadrotor, while the state update of the filter x_{update} represents the predicted value of the filter, and the particle filter

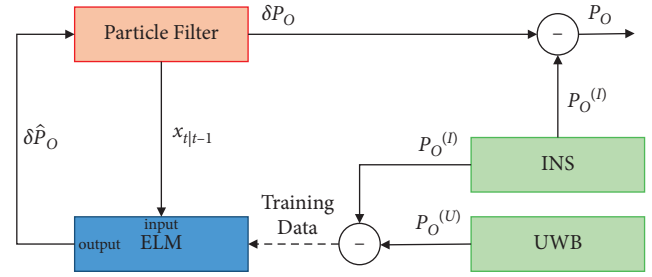


FIGURE 4: ELM provides the observation data-assisted PF process.

outputs the filtering results by comparing the weight relation. The state value x_{state} and state update x_{update} are two different descriptions of the target state, and there are deviations between them, given by

$$\Delta x_t = x_{\text{update},t} - x_{\text{state},t}, \quad (5)$$

where t is the time index. Since the filtering effect will always be affected by the state value, so before the prediction stage, the state deviation Δx should be optimized. According to equation (1) and the real motion model, it can be known that Δx is affected by the previous moment at all moments, that is to say, the present Δx_t is affected by Δx at all previous moments. The (5) is expressed as

$$\Delta x_t = f(\Delta x_{t-1}, \Delta x_{t-2}, \dots, \Delta x_1), \quad (6)$$

where f represents the relational function between them. It should be emphasized that f is unknown, so we use ELM to build this function. In the training model, the quantity of Δx keeps increasing with the change of time, and the training speed of ELM will decline rapidly. We usually set a training scale n to limit the number to the right of (6), for ensuring that the number of states affected by the previous state is the same. So, (6) can be written as

$$\Delta x_t = f(\Delta x_{t-1}, \Delta x_{t-2}, \dots, \Delta x_{t-n}). \quad (7)$$

When $t > n + 2$, the training model is shown in Figure 3.

In the filtering process, when time index $t \geq n + 2$, ELM collects training data $(\Delta x_{t-1-n}, \dots, \Delta x_{t-2}), (\Delta x_{t-n}, \dots, \Delta x_{t-1})$ that are generated by PF as input and output to establish the mapping relationship among them. Then, $(\Delta x_{t-n}, \dots, \Delta x_{t-1})$ as the input of ELM and predict $(\Delta x_{t-n+1}, \dots, \Delta x_t)$ through mapping established in the previous stage. The output state deviation array contains Δx_t needed by PF state update at the next moment. Δx_t is corrected by ELM. After entering PF, x_{update} is calculated by (5) to obtain more accurate estimation information. The process is then repeated until filtering is complete. Thus, the state value of PF is constantly updated by ELM, and the current state value is jointly determined by the previous multiple state values, so the influence of noise is reduced and the positioning accuracy is improved.

4.2. Scheme 2: Replenish Measurement Information When UWB Interrupted. Complicated or hostile indoor environment may lead to the interruption of UWB's signal, and the



FIGURE 5: The quadrotor used in the experiment.



FIGURE 6: The test environment.

observation vector δPo of PF will not be available. Before signal interruption, UWB provides observation data, and ELM is used to establish the mapping between δPo and state value $\hat{x}_{t|t-1}, t \in [1, +\infty)$ output by PF. As in the previous section, this functional relationship is difficult to describe with exact mathematical equations. We use $\hat{x}_{t|t-1}$ as the input training data of ELM and δPo as the training target, ELM through a certain amount of data training to establish the mapping relationship between them. In this way, in the absence of UWB's signal, ELM can predict $\delta \hat{Po}$ through the $\hat{x}_{t|t-1}$ and mapping relationship, so that the filter can work normally and ensure the stability of the system. It should be noted here that among the training data used, the $\hat{x}_{t|t-1}$ output by the filter is obtained through the assistance of ELM, so it is more accurate than the simple PF.

ELM provides the observation data-assisted PF process when UWB measurement is interrupted as shown in Figure 4.

During the training stage, when UWB measurement $Po^{(U)}$ is available, PF provides $\hat{x}_{t|t-1}$. The observation vector $Y_t = [d_t^{(I)} - d_t^{(U)}]$ is the training target and ELM establishes offline mapping through training. In the prediction stage, $Po^{(U)}$ of UWB is not available at this time, ELM predicts $\delta \hat{Po}$ by input $\hat{x}_{t|t-1}$ and mapping relationship instead of Y_t , and PF works normally by using $\delta \hat{Po}$ provided by ELM.

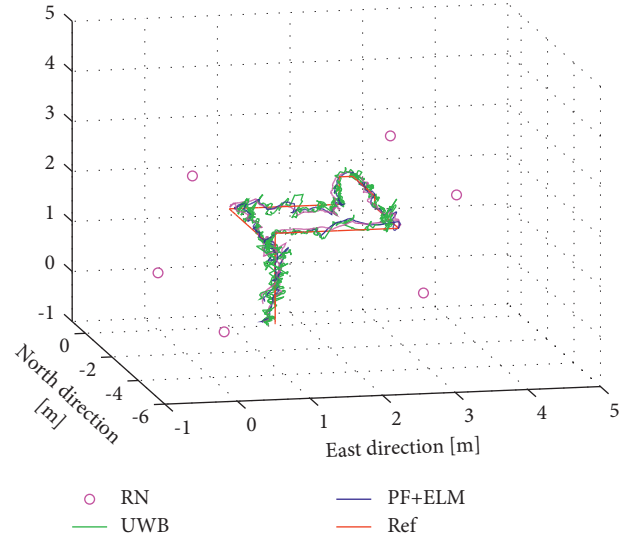


FIGURE 7: The trajectory comparison.

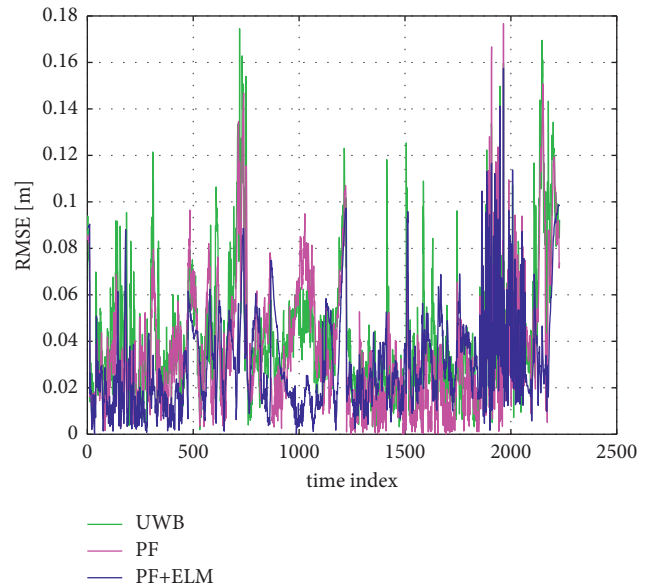


FIGURE 8: RMSE comparison of UWB, PF, and PF + ELM.

5. Test

In order to verify the effectiveness of the proposed strategy, a real experiment has been designed. The availability of the proposed strategy is proved by results of the simulation and error analysis.

5.1. Experimental Settings. The experimental site was selected in an empty space, and (x, y, z) represents the actual directions east, north, and up. The quadrotor is equipped with the inertial measurement unit (IMU) and UWB blind node (UWB BN) to provide reference for distance information. The quadrotor used in the experiment is shown in Figure 5. In order to better position the quadrotor, six UWB

TABLE 1: Average RMSES produced by PF and PF + ELM in the east, north, and up.

	RMSE (m)			Mean	Improving
	East	North	UP		
UWB	0.0692	0.0996	0.0906	0.0864	—
PF	0.0600	0.0909	0.0800	0.0770	10.88 %
PF + ELM	0.0515	0.0768	0.0603	0.0628	27.31 %

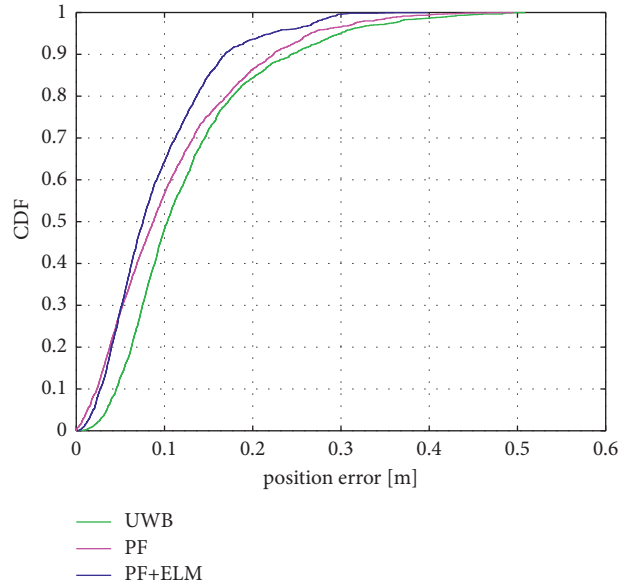


FIGURE 9: CDF comparison of UWB, PF, and PF + ELM.

reference nodes (UWB RNs) were placed at known coordinate points. Three were placed high and three were placed low (height 2.7 m and 0.1 m, horizontal distances between each UWB RN were 2.3 m and 4.6 m, as shown in yellow, $i = 1 - 6$). The UWB RN form a 3D space in which the target quadrotor moves along a planned path. The upper computer collects INS and UWB's data at an interval of $\Delta T = 0.02S$. The actual test scene is shown in Figure 6.

5.2. Localization Errors. In this part, the effectiveness of the proposed strategy is verified by simulation calculation:

Scheme 1: ELM-assisted PF can effectively reduce positioning error

Scheme 2: when UWB's signal is interrupted, ELM compensates the signal through the mapping relationship to make the filter work normally

5.2.1. Error Analysis of Scheme 1: Correction of State Deviation. For scheme 1, the position information $Po^{(I)}$ of INS and $Po^{(U)}$ of UWB can be calculated, respectively, through the data collected by the upper computer, and the flight trajectory in 3D space can be fitted out. The ELM-assisted PF algorithm mentioned in scheme 1 is used to process the data to reduce the influence of bad noise and improve the positioning accuracy. Here, an individual PF

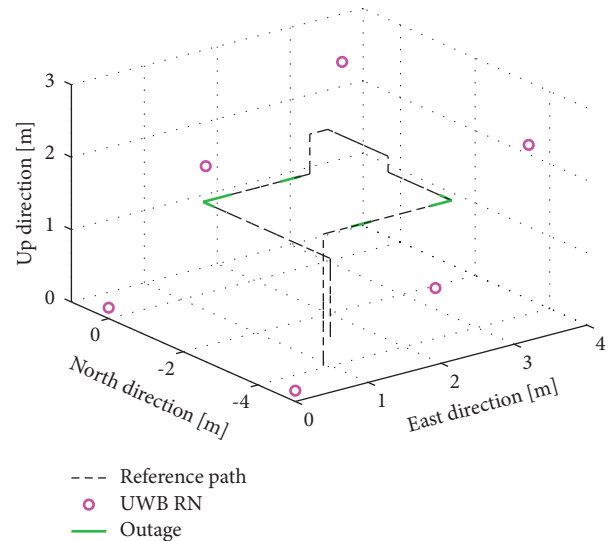


FIGURE 10: Reference trajectory and outage areas (#1, #2, #3, #4).

algorithm is also used to prove the superiority of the proposed strategy by comparison. The trajectory comparison diagram is shown in Figure 7.

The error reduction of the ELM-assisted PF model with that of individual PF was compared. The root mean square error (RMSE) has been used in the x , y , and z directions at all time indexes, which was calculated as

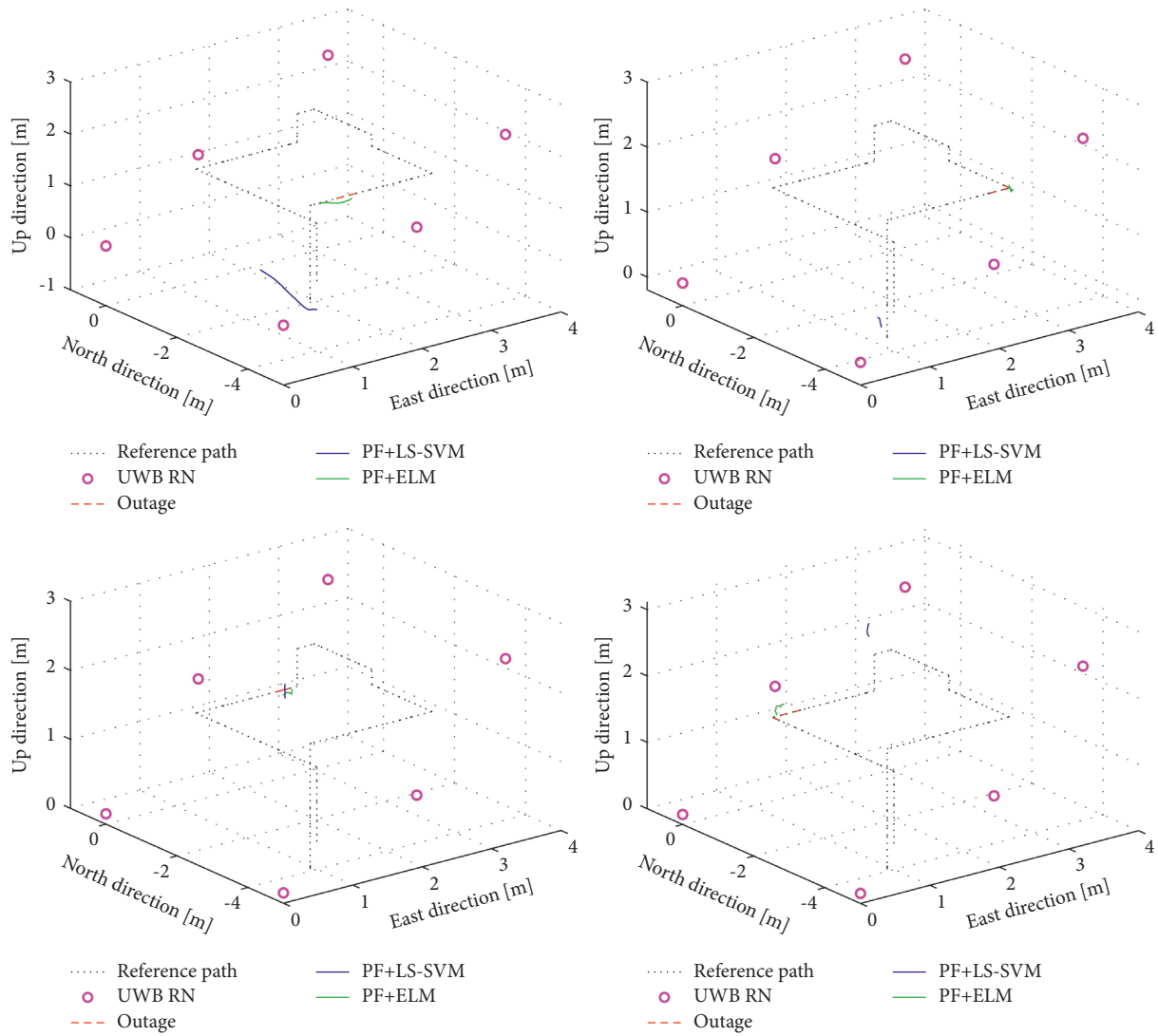


FIGURE 11: Comparison of ELM and LS-SVM prediction values in outage areas.

$$\text{RMSE}(Po)_t = \frac{1}{3} \left(\left((x_t - x_t^{ref})^2 + (y_t - y_t^{ref})^2 + (z_t - z_t^{ref})^2 \right)^{1/2} \right), \quad (8)$$

where $\text{RMSE}(Po)_t$ means the RMSE of the position at time index t , (x_t, y_t, z_t) is the estimated position in x , y , and z directions, and $(x_t^{ref}, y_t^{ref}, z_t^{ref})$ is the reference position in x , y , and z directions at the time index t .

After filtering, RMSE of UWB, PF, and ELM-assisted PF were calculated, and the results are shown in Figure 8 and Table 1.

In Table 1, mean represents the average value of the errors in the three directions. It can be seen that comparing with UWB, the PF algorithm error is reduced by 10.88% and the PF + ELM algorithm error is reduced by 27.31%. Compared with the PF algorithm, PF + ELM algorithm error is reduced by 18.44%. It should be emphasized that UWB positioning and PF are quite exact.

Otherwise, the cumulative distribution function (CDF) is also used to describe the achievement rate of each

algorithm. The comparison of CDF is shown in Figure 9. As shown in the figure, the PF + ELM strategy achieves the ideal state faster than PF alone, indicating that for the INS/UWB combined navigation model, scheme 1 has a better effect on reducing noise and optimizing accuracy.

5.2.2. Error Analysis of Scheme 2: Replenish Measurement Information. For scheme 2, after the position information $Po^{(I)}$ of INS and $Po^{(U)}$ of UWB are fitted, four interrupt regions (#1, #2, #3, #4) were set to simulate the interruption of UWB's signal, as shown in Figure 10.

To demonstrate the performance of the proposed strategy, LS-SVM was also used. In the outage area, ELM and LS-SVM perform signal compensation, respectively, as shown in Figure 11. Meanwhile, RMSEs of four areas are calculated, respectively, according to (8), as shown in Figure 12 and Table 2.

As shown in Figure 11, the red line represents the outage areas of the reference trajectory, the green line represents the

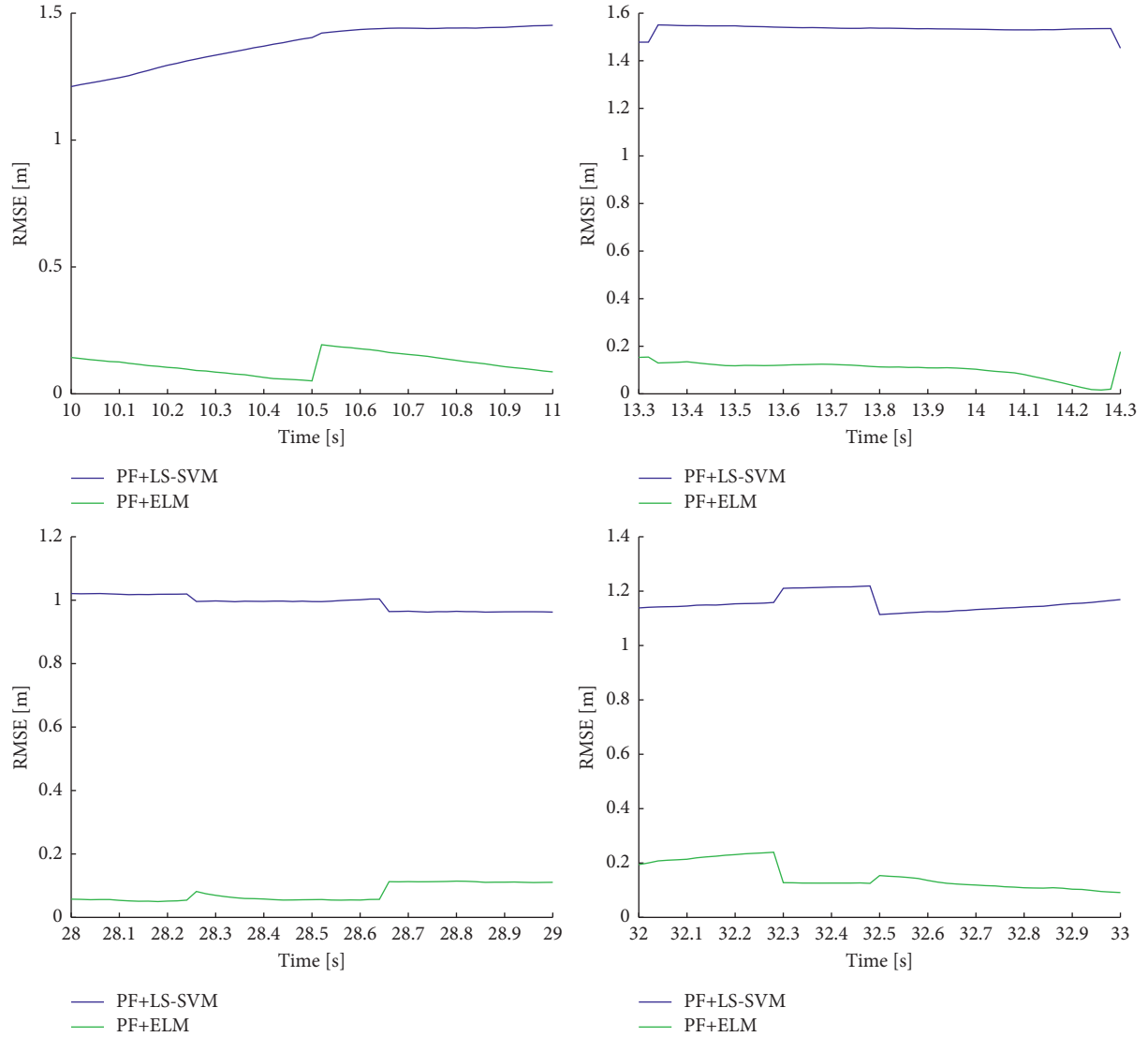


FIGURE 12: The RMSEs estimated by ELM and LS-SVM in outage areas.

TABLE 2: Average RMSEs produced by ELM and LS-SVM in outages #1, #2, #3, #4.

	RMSE (m)				Mean
	#1	#2	#3	#4	
PF + LS-SVM	1.3742	1.5339	0.9910	1.1561	1.2638
PF + ELM	0.1176	0.1046	0.0767	0.1502	0.1123

result of ELM-assisted PF prediction, and the blue line represents the result of LS-SVM prediction. (a), (b), (c), (d) indicate the outage areas #1, #2, #3, #4. Obviously, the difference between PF + ELM and the reference value is smaller, proving that compared with LS-SVM, the proposed strategy is more effective. According to Table 2, the error of PF + ELM is reduced by 1.15 m compared with LS-SVM.

6. Conclusion

In this study, ELM-assisted PF for INS/UWB combined navigation quadrotor positioning strategy is studied. In this

scheme, INS and UWB acquire the position information of the motion quadrotor, respectively, PF performs data fusion and filtering, and ELM is used to assist the filter. ELM establishes the mapping between the difference deviation of each state in the filtering process to correct state deviation. Meanwhile, during the normal operation of PF, ELM keeps training and establishing the relationship between the state vector output by PF and the observation vector. When UWB's signal is interrupted, the observation vector fails; under this condition, ELM makes signal prediction and provides observation signal to make the filter work normally. The experimental results show that the proposed ELM-

assisted PF strategy can effectively correct the state deviation, further reduce the position error on the basis of PF, and improve the positioning accuracy by 18.44% compared with single PF. When the signal is abnormal, PF can also work normally through the observation vector provided by ELM. Compared with LS-SVM, the positioning accuracy provided by ELM improved by 1.15 m.

Data Availability

The data used to support the findings of this study are available from the corresponding author upon request.

Conflicts of Interest

The authors declare that they have no conflicts of interest.

Acknowledgments

This research was supported by the National Key R&D Program of China (2018AAA0101703) and Shandong Provincial Natural Science Foundation (ZR2020KF027).

References

- [1] J. E. Sierra-García and M. Santos, "Intelligent control of an uav with a cable-suspended load using a neural network estimator," *Expert Systems with Applications*, vol. 183, p. 115380, 2021.
- [2] M. Wang, B. Chen, and C. Lin, "Prescribed finite-time adaptive neural trajectory tracking control of quadrotor via output feedback," *Neurocomputing*, vol. 458, pp. 364–375, 2021.
- [3] X. Li, J. Zhang, and J. Han, "Trajectory planning of load transportation with multi-quadrotors based on reinforcement learning algorithm," *Aerospace Science and Technology*, vol. 116106887 pages, 2021.
- [4] C. Zhao, D. Wang, J. Hu, and Q. Pan, "Nonlinear model predictive control-based guidance algorithm for quadrotor trajectory tracking with obstacle avoidance," *Journal of Systems Science and Complexity*, vol. 34, no. 4, pp. 1379–1400, 2021.
- [5] L. Xi, Z. Peng, L. Jiao, and B. M. Chen, "Smooth quadrotor trajectory generation for tracking a moving target in cluttered environments," *Science China Information Sciences*, vol. 64, no. 7, pp. 1–16, 2021.
- [6] Li You, S. Zahran, Z. Yuan et al., "Imu/magnetometer/barometer/mass-flow sensor integrated indoor quadrotor uav localization with robust velocity updates," *Remote Sensing*, vol. 11, no. 7, pp. 838–860, 2019.
- [7] P. Liu, M. N. Huda, L. Sun, and H. Yu, "A survey on underactuated robotic systems: bio-inspiration, trajectory planning and control," *Mechatronics*, vol. 72, p. 102443, 2020.
- [8] M. N. Huda, P. Liu, C. Saha, and H. Yu, "Modelling and motion analysis of a pill-sized hybrid capsule robot," *Journal of Intelligent and Robotic Systems*, vol. 100, no. 3, pp. 753–764, 2020.
- [9] P. Liu, G. Neumann, Q. Fu, S. Pearson, and H. Yu, "Energy-efficient design and control of a vibro-driven robot," in *Proceedings of the 2018 IEEE/RSJ International Conference on Intelligent Robots and Systems (IROS)*, pp. 1464–1469, Madrid, Spain, October 2018.
- [10] Q. Fan, Y. Wu, J. Hui, L. Wu, Z. Yu, and L. Zhou, "Integrated navigation fusion strategy of ins/uwb for indoor carrier attitude angle and position synchronous tracking," *The-ScientificWorldJOURNAL*, vol. 2014, pp. 215303–13, Article ID 215303, 2014.
- [11] Y. Lu, J. Yi, He Liang, X. Zhu, and P. Liu, "A hybrid fusion algorithm for integrated ins/uwb navigation and its application in vehicle platoon formation control," in *Proceedings of the 2018 International Conference on Computer Science Electronics and Communication Engineering*, 2018.
- [12] J. Liu, J. Pu, L. Sun, and Z. He, "An approach to robust ins/uwb integrated positioning for autonomous indoor mobile robots," *Sensors*, vol. 19, no. 4, p. 950, 2019.
- [13] Q. Fan, B. Sun, Y. Sun, Y. Wu, and X. Zhuang, "Data fusion for indoor mobile robot positioning based on tightly coupled ins/uwb," *Journal of Navigation*, vol. 70, no. 5, pp. 1079–1097, 2017.
- [14] Y. Xu, J. Cao, Y. S. Shmaliy, and Z. Yuan, "Distributed kalman filter for uwb/ins integrated pedestrian localization under colored measurement noise," *Satellite Navigation*, vol. 2, no. 1, pp. 305–314, 2021.
- [15] S. T. Ahmad, T. M. R. Khan, and W. B. Yousuf, "Auxiliary particle filter-based multisensor data fusion for quantification of corrosion in aerostructures," *Journal of Testing and Evaluation*, vol. 49, no. 3, pp. 1503–1515, 2019.
- [16] N. Zhou, L. Lau, R. Bai, and T. Moore, "A genetic optimization resampling based particle filtering algorithm for indoor target tracking," *Remote Sensing*, vol. 13, no. 1, p. 132, 2021.
- [17] G. S. Kushwah and S. T. Ali, "Distributed denial of service attacks detection in cloud computing using extreme learning machine," *International Journal of Communication Networks and Distributed Systems*, vol. 23, no. 3, pp. 328–351, 2019.
- [18] P. Niu, Y. Ma, and G. Li, "Model nox emission and thermal efficiency of cfbb based on an ameliorated extreme learning machine," *Soft Computing*, vol. 22, no. 14, pp. 4685–4701, 2018.
- [19] Y. Yi, S. Qiao, W. Zhou, C. Zheng, Q. Liu, and J. Wang, "Adaptive multiple graph regularized semi-supervised extreme learning machine," *Soft Computing*, vol. 22, no. 11, pp. 3545–3562, 2018.
- [20] Z. Liouane, T. Lemlouma, P. Roose, F. Weis, and H. Messaoud, "An improved extreme learning machine model for the prediction of human scenarios in smart homes," *Applied Intelligence*, vol. 48, no. 8, pp. 2017–2030, 2018.